MOSAICKING OF HIGH-RESOLUTION BIOMEDICAL IMAGES ACQUIRED FROM WIDE-FIELD OPTICAL MICROSCOPE

V. Ulman*

* Laboratory of Optical Microscopy, Masaryk University, Brno, Czech Republic

xulman@fi.muni.cz

Abstract: Large 2D high-resolution color images were acquired from wide-field optical microscope. The specimen was from the field of pathology of tissues. Each large image was obtained by stitching from a grid of smaller images. Separate acquisitions required registration and stitching of adjacent images. The novel use of special order for registration allows for easy processing of images with solely background. The order is determined from graph representation based on the grid. In this way, a reliable registration confidence test could be provided. The final large image was composed by stream stitching process because of imposed memory limitations. The stitches between adjacent images themselves were hidden by meandering technique. The methodology is described and several aspects are discussed in this paper. Our experience, gained from practical application of our system in the department of tissue pathology, supports the claim that the system is robust, fast and accurate.

Introduction

Digital microphotography becomes more and more popular in pathology of tissues. One of few enhancements we gain from transition into digital world is the possibility to acquire *large* 2D images at high resolution. Such big images can be annotated and stored into a database as reference images. High-detailed reference images can be used, for instance, when examining another data, for teaching purposes or even in tele-pathology.

We were acquiring high-resolution 2D color images from optical microscope by composing smaller images (fields) of specimen. This solution enables us to acquire every field at the limits of given optical setup, namely at high magnification and resolution possible. The fields were arranged into an orthogonal grid spreading over the entire region of interest of a given specimen.

Nevertheless, high lateral resolution of attached CCD camera is better than the resolution of the movement of mounting stage. This and the mechanical matter of stepper motors implies that the lateral movement of specimen is not described sufficiently at the resolution of fields (images). Adjacent fields were therefore acquired with small overlap providing information for correct alignment of fields.

Another issues stem from the thickness of specimen and from the almost-perpendicularity of specimen plane. The system had to refocus on every field. Due to this and the imperfection of optics, the overlaps of adjacent fields were not exactly identical and some smoothing had to be performed while stitching fields.

The registration was even more complicated because of the structure of specimen. There were fields displaying solely background due to a hole in the specimen or non-convex shape of it. Determining the correct alignment of such fields is hardly possible even for operating personal.

Last, but not least, constraint required a really large mosaicked image (e.g. more than 1GB) to be created using a computer with much less of physical memory (e.g. 0.5GB).

Materials and Methods

The specimen samples were mounted on a 2D moving stage (Märzhäuser, Germany) and acquired with CCD Nikon DXM 1200 camera (Nikon, USA), microscope Leica DMLB (Leica, Germany) with 10x to 100x objectives (lens HC PIApo 10/0.4, HC PIApo 20/0.7, HCX PIApo 40/0.85 CORR and HCX PIApo 100/1.35 Oil Imm). The system is driven by Lucia DI software (Laboratory Imaging, Czech Republic). Fields, comprising a grid, are acquired row by row, each odd row from left to right while each even row from right to left — a meandering scan.

Lucia DI software refocused at each particular field. Sometimes to get a sharp picture, a stack of images was acquired in which each image was focused at different distance. Montage from focused parts of images from 3D stack was conducted resulting in 2D sharp field.

Thus, grid coordinate of each field was known. All fields had the same dimension, typically 1232×972 pixels, and all were in 24-bit colors. Adjacent fields were acquired with overlap, typically 5–10 percent of the field dimensions.

After the acquisition, all fields were stored into separate files and ready for further three-step processing. The goal was to determine a good order for processing of fields as well as to register adjacent fields resulting in global pixel coordinates attached to every field. Coordinates were then used in the final third step where sort of stream stitching process was creating final large image.

Let us denote a set Im to be the set of all fields and $Sur[i]$, $i \in Im$, to be the set of all adjacent fields, i.e. fields

ISSN: 1727-1983

that are, if they exist, to the left, top, right and bottom relative to the given field *i*. A set of pixel coordinates, in the coordinate system of field *i*, of a part corresponding to overlap between fields *i* and *j* is designated as $part_{i\to j}$. Coordinates of the most right pixel line and the most bottom pixel line are excluded from the set for the sake of equation (2). Pixel value of field *i* at coordinate (x,y) will be $p_i(x,y)$.

Boundary *parts* of every field were converted into 8-bit grayscale and stored into computer memory. A *part* is actually an edge of a boundary frame of an image. It is slightly wider than the overlap that was used during acquisition of individual fields. It was expected that every part contained the real overlap. Some parts are outlined in Figure 1 by dashed lines.

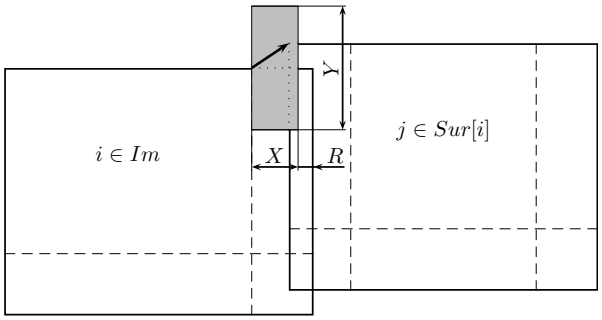

Figure 1: Parts and possible alignments

The registration order is established from weighted graph representation (Im, Mes) of the grid. Vertices of the grid are fields themselves, the set *Im*. Edges are just between two adjacent vertices (fields). The weight of every edge is described by $Mes[i \leftrightarrow j], \forall i \in Im, \forall j \in Sur[i]$. Modified Prim algorithm for finding maximum spanning tree is used, Figure 2. It is the order, in which fields are

(1) for $\forall i \in Im$ do $Pr[i] := 0$ and $Val[i] := -\infty$
(2) $i' := \max_{i\in Im}\left(\sum_{j\in Sur[i]} Mes[i \leftrightarrow j]\right)$
(3) while $\exists i \in Im : Pr[i] = 0$ do
(4) for $\forall j \in Sur[i'] : Pr[j] = 0 \wedge Val[j] < Mes[i \leftrightarrow j]$ do $Val[j] := Mes[i \leftrightarrow j]$
(5) $Pr[i'] := 1$, PRINT(i')
(6) $i' := \max_{i\in Im:Pr[i]=0}(Val[i])$
(7) end while

Figure 2: Modified Prim algorithm

printed in the given algorithm (step (5)), that is used for fields registration and computation of global pixel coordinates. The weight is given by equations (1) and (2):

$$Mes[i \leftrightarrow j] = Mes[i \to j] + Mes[j \to i], \qquad (1)$$

$$Mes[i \to j] = \sum_{(x,y)\in part_{i\to j}} |p_i(x,y) - p_i(x+1,y)| + \sum_{(x,y)\in part_{i\to j}} |p_i(x,y) - p_i(x,y+1)|. \qquad (2)$$

The correct alignment of two adjacent fields was established by voxel-based registration methods [1, 2]. These methods test all reasonable alignments, the $X \times Y$ area in Figure 1, and evaluate each of them. The best alignment should have the highest evaluation. In our implementation, the search for translation of corresponding parts was just enough. The result of registration was a two-elements vector, thick arrow in Figure 1, estimating the best alignment of two adjacent fields.

Two *default* vectors were maintained, one for horizontal and one for vertical alignments. The very first registration in given direction determined the default vector for that direction. Every consecutive successful registration in the same direction improved the respective default vector. Improvement was done via re-averaging so far computed successful registration vectors in given direction. Registration was considered successful whenever the found registration vector did not differ more than 10 pixels from default vector in some of its elements. Otherwise, the found vector was ignored, default vector was supplied and no improvement was calculated.

Searching the alignment space was reduced by two optimization techniques. The very first search in given direction was improved using *n*-step optimization technique. First, this technique tests every *n*-th alignment among all from those in $X \times Y$. Then, it searches every $(n/2)$-th alignment in a $n \times n$ surroundings of the, so far, highest evaluated alignment. The last step repeats with $n := n/2$ and ends when $n = 1$. After the default vector for given direction was established, every consecutive search was optimized using gradient ascend technique. In this case, the search starts with the default vector. Neighboring vectors are examined and the highest one is selected for the next iteration. The iteration stops whenever no better alignment is around.

Global coordinates of the top left corner of every field $i \in Im$ were determined immediately when alignment vectors between *i* and all $j \in Sur[i]$ were computed. The global coordinate $(0,0)$ was in the top left corner of the field i' determined in the step (2). The modified Prim algorithm (Figure 2) ensures the property that whenever global coordinate of *i* is being computed, there exists at least one field from $Sur[i]$ that has its global coordinate already established allowing to set the global coordinate of *i* in this way.

Global coordinates of every top left corner were used when creating final large image. The original 24-bit color images (fields) were loaded into memory from a given grid line and stitched together according to associated global coordinates. The first two grid lines were assembled separately and stitched together. Then, as much as possible pixel lines were stored into the output image file (and removed from memory). The third grid line was assembled and stitched with the rest of the first two grid lines. The process was repeated by storing as much pixel lines as possible and proceeding with next grid line until all grid lines are processed.

A smooth transition within an overlap was utilized.

ISSN: 1727-1983

Horizontal transition between fields occurred when assembling a grid line and vertical transition occurred when stitching two grid lines. Transition was implemented as weighted sum of both intensities of corresponding pixels. The weights were controlled by two continuous functions: one was smoothly lowering influence of image data while another was raising influence of the counterpart image data.

Results

We have tested five registration methods, namely the stochastic sign change (SSC), the sum of absolute valued differences (SAVD) [1], the normalized cross-correlation coefficient (NCC) [1, 3, 4], the correlation ratio (CR) [5, 6] and mutual information [7, 8]. Two versions for estimation of underlying pixel intensity probability densities in mutual information method were tested: estimation from joint histogram (MI_h) [9] and estimation using Parzen estimator (MI_P) [10]. The time consumption of tested registration techniques is presented in Table 1 where each value (time) is for the same particular registration. The last column was measured on different registration in the same grid since the used default vector was the result from previous columns.

Table 1: Speed comparison of registration techniques

	Entire search	4-step tech.	8-step tech.	16-step tech.	Gradient ascend
SSC	55.323s	3.372s	1.027s	0.465s	0.031s
SAVD	44.746s	2.701s	0.821s	0.369s	0.036s
NCC	63.568s	3.995s	1.215s	0.546s	0.050s
CR	74.594s	4.746s	1.441s	0.648s	0.060s
MI_h	121.567s	7.835s	2.296s	0.990s	0.085s
MI_P	873.925s	56.460s	15.468s	5.384s	0.352s

The most important observations were, perhaps, the robustness of voxel-based registration methods and the movement behavior of the mounting stage. Tested registration methods proved that it is enough to search on just grayscaled data for correct alignment. This introduced big memory savings since parts could have been stored in just grayscale. Furthermore, all methods except MI_P exhibited smooth evaluation of alignments and performed equally well under normal circumstances. The smoothness is illustrated in Figure 3 where x and y axes constitute a region in a plane of evaluated translational vectors. Each vector represents unique alignment. The vertical axis describes the evaluation. Domain of tested alignments is demonstrated in Figure 1, where the registration of adjacent fields in a grid row is outlined, in the gray area. Using the notation from both figures it holds $(x,y) \in X \times Y$. The $R \times Y$ area was excluded from evaluation. In this particular example of Figure 3 the overlap was set to 7%. Thus, it was: $X = \langle 0, 76 \rangle$, $R = \langle 77, 86 \rangle$ and

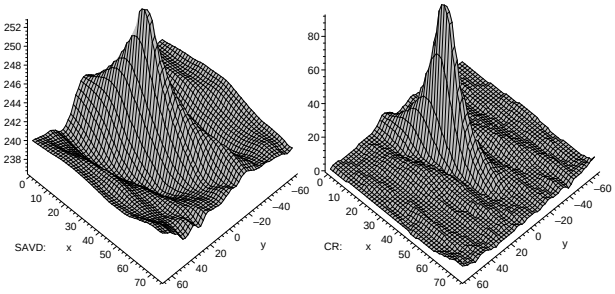

Figure 3: Alignment evaluation

$Y = \langle -68, 68 \rangle$. The smoothness enabled us to make use of optimization techniques which introduced acceleration that can be seen in Table 1.

The observed distribution of translational vectors in given direction resembled normal distribution. This was in agreement with expected behavior of moving stage because the controlling software always made it move by exactly the same number of distance units. Small fluctuations about mean value are due to better lateral resolution of the optical setup. The aim of default vector, for the direction under consideration, was to estimate the mean value of the stage. This reasoning enabled us to use the default vector as a starting alignment for gradient ascend optimization technique which, in fact, only refined the registration for given situation.

The robustness of registration technique and the default vectors provided the solution for detection of registration failures. It occurred, from time to time, that registration of two adjacent fields failed. Typically, the background formed more than two-thirds of overlap or there were at least two equally probable alignments — graphs, as those in Figure 3, contained more than two peaks. The deviation from expected behavior was detected using default vector as described in the previous section.

The registration order was very important because of default vectors estimation. We were successful with modified Prim algorithm, Figure 2, which builds a maximum spanning tree on the most robust edges — robust from the registration point of view. The robustness was indicated by the measure given by equations (1) and (2). The proposed measure emphasized overlaps with non-constant texture that displayed some edges (i.e. structure) which, in turn, was expected to guide the registration process. Especially, the measure was low for overlaps with background only. The ordering for highly-scattered non-convex specimen acquired using a grid of 10×9 fields is demonstrated in Figure 4. Every field is designated by its field coordinate and its number according to registration order. Fields, with its coordinate depicted in a frame, were among thirty fields that had its global coordinates established first.

A transition smoothing was performed when stitching adjacent fields. Since the overlap data were not strictly identical, a simple overlay of, say, left field over right field was not satisfactory. Notice the right-hand side of Figure 5A where the overlay is noticeable. The direction

ISSN: 1727-1983

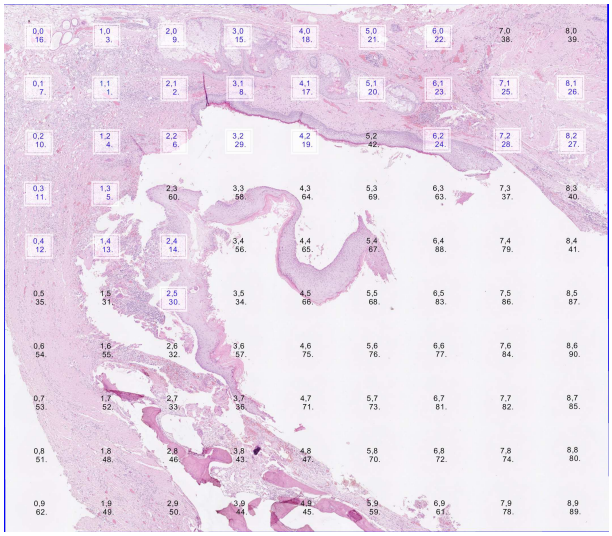

Figure 4: Mosaicked image and the registration order

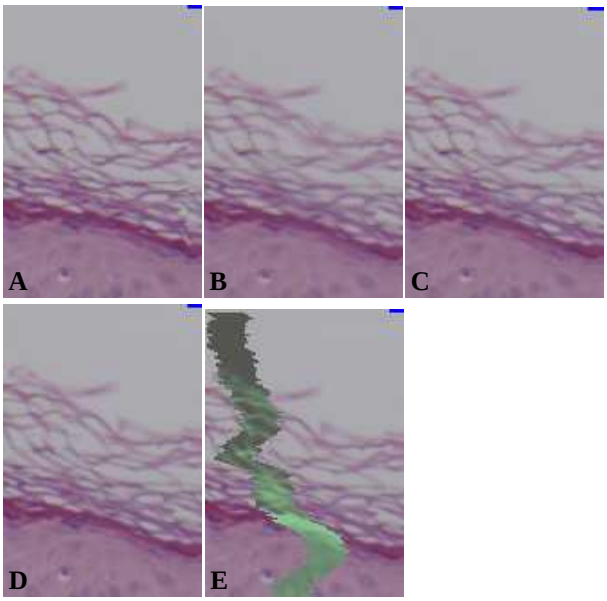

Figure 5: Demonstration of few transition techniques

of transition is horizontal in Figure 5. Also note that the overlay can be implemented as weighted sum with one weight function constant at value 1 and another weight function constant at value 0. A slightly better adjustment of weights represented the linear weight function ranging from 1 to 0 and from 0 to 1, respectively, over the entire overlap. Pitfall of such smooth transition is visible in the middle vertical stripe of overlap in Figure 5B. A kind of blurring is visible there due to similar values of both weight functions and due to data shift induced by non-identical overlap data. We got better outcome by using quadratic or even biquadratic weight functions (ranging again from 1 to 0 and vice versa), Figure 5C. Such weights performed more rapid and yet smooth transition making the blurred stripe narrower thus less noticeable. A “zig-zag” technique further improved the outcome of polynomial weights by narrowing the transition stripe, in our implementation to 20 pixels, and by letting it to meander along the axis perpendicular to transition direction. Result of this technique is shown in Figure 5D. Visualization of meandering transition stripe is in Figure 5E.

The stream stitching of fields was selected because of memory constraint. It also holds a pleasant property, from the implementation point of view, enabling to always stitch along the whole edge of adjacent fields or adjacent assembled grid lines. Furthermore, this property also determines the minimum memory requirement. The memory subsystem must be able to store at least two grid lines of entire input 24-bit color images (fields). Depending on image dimensions and the size of overlap, this requirement was more demanding than the requirement to store, at the moment, all 8-bit grayscale parts from all fields in a memory subsystem.

Discussion

The nature of pathological specimen, which typically displays some tissue, predetermines the voxel-based registration methods. Tissues hardly ever contain some specific features that can be extracted. Furthermore, these features should be present within overlaps of all adjacent fields. Consequently, the feature-based registration techniques are out of question.

Voxel-based techniques proved to handle images of tissues well. Unfortunately, the search through the parameter space is really time demanding. Even in spite of the fact that we search only for translational vectors (i.e. two dimensional space). In our particular experiments the evaluation of alignments behaved well which enabled us to use optimization techniques. In this way, we were able to outweight the time consumption and gain a really fast implementation.

However, in general case, we cannot be confident of the shape of the alignment evaluation of an arbitrary data without any prior analysis. An example of a shape of an evaluation is in Figure 3. Moreover, the Gaussian property of moving stage cannot be expected in advance either. In such situations we always have to search the entire registration parameter space. If the shape of evaluation is smooth then we may use the n-step optimization technique to speed up the registration process since it is quite a general optimization technique (it resembles classical pyramidal approach to search for global extrema). A huge speed up can be gained even for small n, i.e. $n = 4$, while the base diameter of peak is usually larger than basic step. Still, we may remain helpless without the Gaussian property of moving stage — for instance, when the shape of evaluation is not unimodal.

The Gaussian property of moving stage allowed us to handle fields where registration was not clear. We tested the reliability of registration by computing deviation from default vector which estimated the mean movement of moving stage for that particular direction. This solution worked well. We could have used weights

ISSN: 1727-1983

from described graph representation to detect potential registration-failure fields instead. But we would still have to decide what to do with such fields, how to determine the global coordinates. In our approach the default vectors become handy in such situations. We also believe, though we have not tested, that detection of successful registration by deviation from default vector is more powerful since it is not based directly on specific image data. In fact, the detection of failure is based on the behavior of registration.

The order establishment is crucial for setting the default translational vectors. In our implementation the responsibility is on the measure given by equations (1) and (2). The measure should represent the applicability of given overlap to image registration procedure. The higher the measure is the more information the part poses which is expected to be better for registration methods. The adjacent fields with background in their overlap are less weighted than fields with tissue in overlap since the background is expected to be more uniform. The texture of background is more solid with a few noticeable pixel intensities changes in comparison to texture of arbitrary tissue.

The aim of transition was to preserve the original information as much as possible. The stitching process left original data untouched and moved into adjacent image data as fast as possible. A small area of entire overlap was computed from both image data which typically resulted in a decent blur. We've adopted this solution because of streaming nature of final large image composition which, again, enabled us to work with whole field's edge or assembled grid line.

Conclusions

We have described a software solution for obtaining large 2D color images in high-resolution microscopy. For this purpose we developed a special program which can run very fast while still accurate as much as possible. The entire system can efficiently make use of digital microscope and an ordinary personal computer for acquiring large-scale high-resolution color images of pathological specimen.

However, the presented methodology doesn't have to work on general image mosaicking problem satisfactorily. For example, we are expecting the orthogonal grid of fields, which may pose a strong requirement in general, although it is quite natural in microscopy. The selection and processing order of techniques was focused on microscopy of tissues. The parameters of techniques were tuned for particular optical setup. We tried to discuss some aspects of our solution and suggest what to do when some of expected constraints are not met.

The system is still in use in The Faculty Hospital Brno in combination with Lucia DI software. The mosaicking process itself works fully automatic on several different kinds of tissue. The registration in combination with default vectors computes global coordinates well in respect to the stitching. The smoothed transition was not deemed harming by pathologists. The stitching process, as described, didn't produce any artifacts that could violate the analysis.

Acknowledgements

Presented work has been supported by the Ministry of Education of the Czech Republic (Grant No. MSM-0021622419).

References

[1] ČAPEK M. (1999): 'Registrace snímků z konfokálního mikroskopu', (Czech Technical University, Prague)
[2] BROWN, L. G. (1992): 'A survey of image registration techniques', (Columbia University, New York)
[3] BUDÍKOVÁ M., MIKOLÁŠ Š., and OSECKÝ P. (1998): 'Teorie pravděpodobnosti a matematická statistika', (Masaryk University, Brno)
[4] BOURKE P. (1996): 'Cross correlation', Internet site address: http://astronomy.swin.edu.au/~pbourke/analysis/correlate
[5] ROCHE A., MALANDAIN G., PENNEC X., and AYACHE N. (1998): 'Multimodal image registration by maximization of the correlation ratio', (Institut National de Recherche en Informatique et en Automatique, Sophia-Antipolis)
[6] ROCHE A., MALANDAIN G., PENNEC X., and AYACHE N. (1998): 'The correlation ratio as a new similarity measure for multimodal image registration', Proc. of MICCAI 1998, Cambridge, USA
[7] VIOLA, P. A. (1995): 'Alignment by Maximization Of Mutual Information', (Massachuttes Institute of Technology, Cambridge)
[8] VIOLA P. and WELLS III, W. M. (1997): 'Alignment by maximization of mutual information', *International Journal of Computer Vision*, p. 137–154
[9] ZAFFALON M. and HUTTER M. (2002): 'Robust feature selection by mutual information distributions', (IDSIA, Lugano)
[10] GILLES S. (1996): 'Description and experimentation of image matching using mutual information', (Oxford University, Oxford)

ISSN: 1727-1983